

8-1-2013

Stochastic Reconstruction of Multiple Source Atmospheric Contaminant Dispersion Events

Derek Wade
Boise State University

Inanc Senocak
Boise State University

Stochastic Reconstruction of Multiple Source Atmospheric Contaminant Dispersion Events

Derek Wade and Inanc Senocak

*Department of Mechanical and Biomedical Engineering
Boise State University
1910 University Dr. Boise, ID 83725-2085*

Abstract

Reconstruction of intentional or accidental release of contaminants into the atmosphere using concentration measurements from a sensor network constitutes an inverse problem. An added complexity arises when the contaminant is released from multiple sources. Determining the correct number of sources is critical because an incorrect estimation could mislead and delay response efforts. We present a Bayesian inference method coupled with a composite ranking system to reconstruct multiple source contaminant release events. Our approach uses a multi-source data-driven Gaussian plume model as the forward model to predict the concentrations at sensor locations. Bayesian inference with Markov chain Monte Carlo (MCMC) sampling is then used to infer model parameters within minutes on a conventional processor. The composite ranking system enables the estimation of the number of sources involved in a release event. The ranking formula allows plume model results to be evaluated based on a combination of error (scatter), bias, and correlation components. We use the 2007 FUSION Field Trial concentration data resulting from near-ground-level sources to test the multi-source event reconstruction tool (MERT). We demonstrate successful reconstructions of source parameters, as well as the number of sources involved in a release event with as many as three sources.

Keywords:

Event Reconstruction, Bayesian Inference, Source Term Estimation, Gaussian Plume Model

1. Introduction

Environmental awareness plays an important role in public safety, health, and threat mitigation. The release of harmful contaminants into the atmosphere could come by intentional or accidental means, and a quick response is key to limiting possible hazard to the population. Researchers have proposed event reconstruction (ER), also called source-term estimation (STE), methods (Annunzio et al., 2012a; Chow et al., 2008; Keats et al., 2007; Senocak et al., 2008; Stohl et al., 1998) that use contaminant concentration data from a network of well-placed sensors to characterize a dispersion event in terms of its source location

9 and emission rate. STE methods have been studied for many applications including defense
10 and air quality management (Watson and Chow, 2004).

11 Most ER models adopt an inverse problem methodology along with a forward model
12 to predict the plume dispersion. In cases where contaminant dispersion takes place over
13 flat terrain on a scale of several kilometers or less, Gaussian plume models have been an
14 effective forward model in ER methods (Senocak et al., 2008; Allen et al., 2007). At the
15 continental scale with variable meteorological conditions, Monache et al. (2008) used the
16 Lagrangian Operational Dispersion Integrator (LODI) as the forward model in a stochastic
17 reconstruction method to determine the location of a radioactive release in Algeciras, Spain.
18 At the urban neighborhood scale, Keats et al. (2007) adopted a computational fluid dynamics
19 (CFD) model to better capture the effects of complex buildings on contaminant dispersion.

20 Researchers have adopted different methodologies to formulate a STE problem. Both de-
21 terministic and probabilistic algorithms have been proposed. By and large Bayesian inference
22 methods form the basis for most of the probabilistic approaches. Johannesson et al. (2004)
23 presented dynamic Bayesian models using both the well-established Markov chain Monte
24 Carlo (MCMC) method and the sequential Monte Carlo for target tracking and atmospheric
25 dispersion event reconstruction problems. Chow et al. (2008) extended the work presented in
26 Johannesson et al. (2004) to neighborhood scale (building-resolved) atmospheric dispersion
27 events using CFD models. Keats et al. (2007) combined a Bayesian inference method with
28 an adjoint approach to reduce the computational time to reconstruct a release event in an
29 urban environment using CFD based models. Senocak et al. (2008) developed a data-driven
30 approach within a Bayesian inference framework whereby empirical turbulence diffusion pa-
31 rameters of the Gaussian plume model are estimated as part of the inverse problem in ad-
32 dition to characterizing the dispersion event. The practice led to substantial improvements
33 over the empirically tuned Gaussian plume model.

34 Some researchers have favored a deterministic approach in which an optimization method
35 is used to solve the inverse problem. Henze et al. (2009) discusses the use of adjoint models
36 to inversely model $PM_{2.5}$ (particles with diameter less than $2.5\mu m$) emissions. Akcelik et al.
37 (2005) describes an optimization method which uses a conjugate gradient method to solve
38 systems of partial differential equations. This method takes advantage of parallel computing
39 to improve speed and efficiency of the otherwise lengthy optimizations for single-source event
40 reconstructions. Another optimization method, proposed by Annunzio et al. (2012b), uses
41 a Genetic Algorithm (GA) to carry out the optimizations in order to determine the source
42 location of a single source release.

43 A contaminant dispersion event can involve releases from multiple sources. The source
44 type may vary (e.g., point, line, area, volume) as well as the source elevation (e.g., ground
45 level, stack, elevated line from aircraft). The release may also be categorized by the manner in
46 which it is released, such as instantaneous (puff), continuous, or time-varying. Based on the
47 methods described in Annunzio et al. (2012b), Annunzio et al. (2012a) introduced the Multi-
48 Entity Field Approximation (MEFA) method for cases involving one or more ground-level
49 point sources. With regards to continuous release scenarios, MEFA uses available wind data,
50 and constrains any multiple releases to fall within a hazard area predicted by calculating the

51 spread far downwind for a single-source plume approximation. MEFA then searches within
52 this hazard area for the optimal source locations while incrementing the number of possible
53 sources. A cost function is used in part to determine the number of sources involved in the
54 dispersion event. Field data is used to show that the method is capable of providing good
55 approximations for multi-source events.

56 Platt and DeRiggi (2012, 2010) analyzed the blind predictions from STE models provided
57 by eight different research groups, as applied to the FUSION Field Trials of 2007 (FFT-07)
58 dataset (Storwold Jr., 2007). The comparative investigation provided useful information as
59 to how well existing STE models perform relative to other STE models under different release
60 scenarios. Platt and Deriggi applied a linear regression analysis to determine the significant
61 factors that affected the reconstruction results obtained from various models. The present
62 Bayesian inference method (Senocak et al., 2008) with a single-source, continuous release
63 capability was also a part of the investigation. A subset of the results has revealed the
64 advantages of a Bayesian inference method over other inverse methods that used the same
65 forward model (i.e. Gaussian plume model).

66 Reconstruction of a multi-source contaminant release event is more challenging than
67 reconstruction of a single source event. Yee has shown remarkable success using Bayesian
68 inference techniques to reconstruct multi-source events with the number of sources unknown
69 a priori (Yee, 2008, 2012a,b). Yee incorporates the unknown number of sources into the
70 Bayesian inference framework in a principled fashion, which results in a posterior probability
71 density for the number of sources. In our approach, we propose an alternative method
72 to source number quantification by extending the Bayesian inference method presented in
73 Senocak et al. (2008) to reconstruct contaminant dispersion events from multiple sources
74 and couple it with a model ranking system. We adopt a data-driven multi-source Gaussian
75 plume model as the forward model in the Bayesian inference method, and suggest a separate
76 ranking system to estimate the number of sources involved in a release event. We apply the
77 combined method to FFT-07 trial cases with up to three sources.

78 2. Forward Model

79 We adopt a data-driven Gaussian plume model as the forward model, because it is a
80 suitable model for short range releases, over flat terrain under steady wind conditions, such
81 as the FFT-07 trials considered in the present study. It is also computationally inexpensive.
82 Therefore it can be used rapidly in the sampling process within the Bayesian approach.
83 We are able to achieve accurate reconstructions in under two minutes on a conventional
84 workstation with an Intel E8400 3.0 GHZ processor. Speed is an important aspect of STE
85 when the intended use is first-response. Sophisticated forward models should be preferred
86 for contaminant dispersion problems where a Gaussian plume model might not be suitable.

87 Stockie (2011) presents a derivation of the Gaussian plume model with single and multiple
88 contaminant sources. For a single source release, the Gaussian plume model can be written
89 as follows:

$$C_m(x, y, z) = \frac{Q}{2\pi U \sigma_y \sigma_z} \exp\left(-\frac{y^2}{2\sigma_y^2}\right) \times \left\{ \exp\left(-\frac{(z-H)^2}{2\sigma_z^2}\right) + \exp\left(-\frac{(z+H)^2}{2\sigma_z^2}\right) \right\}, \quad (1)$$

90 where C_m is the concentration at location (x, y, z) , Q is the rate of emission for the point
 91 source, U is the average wind speed, and H is the height of the release. We set z to 2m, the
 92 same height as the samplers used in the FFT-07 field experiments. In the FFT-07 trials, the
 93 contaminant was released from a near-ground-level source, therefore H is also set to 2m. H
 94 can also be set as an unknown and estimated using the Bayesian inference method as was
 95 shown in Senocak et al. (2008). Additionally, we combine $\frac{Q}{U}$ into a single parameter. The
 96 release rate, Q can then be estimated by calculating an average wind speed from local wind
 97 measurements at sensor height over the duration of the experiment.

98 We use an open-country Pasquill D type stability (Hanna et al., 1982) to define turbulent
 99 diffusion parameters σ_y and σ_z as follows:

$$\sigma_y = \zeta_y x (1 + 0.0001x)^{-0.5}, \sigma_z = \zeta_z x (1 + 0.0015x)^{-0.5} \quad (2)$$

100 where σ_y and σ_z are the standard deviations used in Equation 1 for the horizontal and
 101 vertical plume directions normal to the streamwise plume direction. Here, x refers to the
 102 distance along the streamwise plume direction. The parameters ζ_y and ζ_z are left as unknown
 103 parameters to be estimated by the Bayesian method, making the forward model a data-driven
 104 one. The practice results in significantly better estimates for the concentration field (Senocak
 105 et al., 2008; Senocak, 2010). Data-driven forward modeling gives better predictions than the
 106 baseline forward model when there are sufficient and reliable sensor data.

107 3. Bayesian Inference Method for Multi-Source Release Events

108 The Stochastic Event Reconstruction Tool (SERT) (Senocak et al., 2008) uses Bayesian
 109 inference to estimate information (i.e., source location, release height, emission rate, wind
 110 direction and speed) about the dispersion event. In this section, we present the Bayesian
 111 inference framework in SERT and extend it to multiple source releases. The number of
 112 sources involved in an event is then estimated separately using a ranking formula.

113 Generally speaking, the inverse problem can be formulated as follows:

$$\mathbf{m} \approx F^{-1}(\mathbf{d}), \quad (3)$$

114 where \mathbf{d} is a vector of observed concentration values and \mathbf{m} is a vector of forward model pa-
 115 rameters to be estimated. F is the forward model, which is the Gaussian plume model in our
 116 case. Given the observed data, \mathbf{d} , our goal is to estimate forward model parameters, \mathbf{m} . In
 117 most Bayesian inference methods, Bayes' rule is simplified into the following proportionality:

$$P(\mathbf{m}|\mathbf{d}) \propto L(\mathbf{d}|\mathbf{m})P(\mathbf{m}), \quad (4)$$

118 where $P(\mathbf{m}|\mathbf{d})$ refers to the posterior probability density of the forward model parameters,
 119 $L(\mathbf{d}|\mathbf{m})$ is the likelihood function which calculates the likelihood of the observations given the
 120 model parameters, and $P(\mathbf{m})$ is the prior probability for the model parameters (Congdon,
 121 2010).

122 Prior probabilities for model parameters are set based on certain expectations about each
 123 of the model parameters. All model parameters except Q/U and σ^2 are assigned proper
 124 uniform prior distributions. The normalized emission rate Q/U is given a Jeffrey's prior as
 125 follows:

$$p(Q/U) \propto \frac{1}{Q/U}. \quad (5)$$

126 To avoid division by zero we set a small minimum value for Q/U . Q/U is scaled using this
 127 minimum value to ensure that the maximum prior value is unity.

128 There are sensors capable of detecting trace amounts of a material in the atmosphere.
 129 But they have their limitations. Sensors can register a nominally zero value when, in fact,
 130 local concentration level, d_i , can be non-zero and below the detection threshold of the sensor.
 131 In such cases, we assign a probability to detecting a zero concentration level as follows:

$$d_i = \begin{cases} 0, & \text{with probability } \exp(-\alpha \cdot \hat{C}_i) \\ \xi_i, & \text{with probability } 1 - \exp(-\alpha \cdot \hat{C}_i) \end{cases} \quad (6)$$

132 where ξ_i is a concentration measured by a theoretically ideal sensor, d_i is the concentration
 133 measured by an actual sensor, and \hat{C}_i is the concentration predicted by the model at the
 134 sensor location. Given the model parameters, ξ_i has a lognormal distribution with the
 135 following density:

$$p(\xi_i|\mathbf{m}) = \frac{1}{\sqrt{2\pi}\sigma\xi_i} \exp\left(-\frac{1}{2\sigma^2}(\ln \xi_i - \ln \hat{C}_i)^2\right), \quad (7)$$

136 When a sensor makes an observation at the sensor's detection threshold, C_{th} , we assume
 137 that it does so with a probability of $1/2$. Based on this assumption and Equation 6, α can
 138 be computed in the following manner:

$$1 - \exp(-\alpha \cdot C_{th}) = \frac{1}{2} \rightarrow \alpha = \frac{1}{C_{th}} \ln(2). \quad (8)$$

139 Given Equation 6, the conditional likelihood function is written as follows:

$$L(d_i|\mathbf{m}) = \begin{cases} \exp(-\alpha \cdot \hat{C}_i), & \text{if } d_i = 0 \\ \frac{1 - \exp(-\alpha \cdot \hat{C}_i)}{\sqrt{2\pi}\sigma d_i} \exp\left(-\frac{1}{2\sigma^2}(\ln d_i - \ln \hat{C}_i)^2\right), & \text{if } d_i > 0 \end{cases}, \quad (9)$$

140 where σ^2 , is the variance, which takes into account modeling and measurement errors cumu-
 141 latively. We assume that the variance has an inverse gamma prior distribution with hyper

142 parameters $\alpha = 1.0$ and $\beta = 1000.0$.

143 SERT's previous design focused on single source continuous releases. In this study, we
 144 first modify the forward model to extend SERT to multiple source events. For a multi-
 145 source plume of a non-reactive and non-buoyant contaminant, the concentration at any
 146 point (x, y, z) is the sum of the contributions from each source (Stockie, 2011).

$$C_{total}(x, y, z) = \sum_{s=1}^n C(x'_s, y'_s; Q_s), \quad (10)$$

147 where n is the number of sources, and Q_s is the source emission rate. As in Stockie (2011),
 148 the shifted coordinates, x'_s and y'_s , are defined as follows:

$$x'_s = x - X_s, y'_s = y - Y_s, \quad (11)$$

149 where, x and y are the Cartesian coordinates, X_s and Y_s are the coordinates of source s .
 150 The origin is shifted to the source location, (X_s, Y_s) , and the positive x-direction extends in
 151 the downwind direction.

152 Next, we introduce additional parameters required by the multi-source model into the
 153 Bayesian inference framework. Hereinafter we will refer to the multi-source event reconstruc-
 154 tion tool as MERT. For multiple source releases, we define a reference source, and all other
 155 sources are defined relative to the reference source based on the distance to the source, d ,
 156 and an angle, φ , measured from the global x-axis, as shown in Figure 1. Each source has its
 157 own emission rate normalized by the mean wind speed, $\frac{Q}{U}$. For example, the complete set of
 158 forward model parameters for a dual source model can then be written as follows:

$$\mathbf{m} = \left[x_{s1}, y_{s1}, \left(\frac{Q}{U} \right), \theta, \zeta_y, \zeta_z, \sigma^2, d_2, \varphi_2, \left(\frac{Q}{U} \right)_2 \right], \quad (12)$$

159 where (x_{s1}, y_{s1}) is the primary source location, and θ is the wind direction. We use Markov
 160 chain Monte Carlo (MCMC) sampling with the Metropolis Algorithm (Metropolis et al.,
 161 1953) to estimate the posterior distribution of the model parameters. In our approach, the
 162 candidate state is sampled from a Gaussian distribution centered on the current state.

163 Figure 1 shows a dual source plume with sufficient distance between two sources, such
 164 that overlap of the plumes does occur downstream and yet the sources are not too close
 165 together to consider them as a single entity. We assume that the distance between the two
 166 sources, d , is relatively small compared to the size of the search region. Therefore, for the
 167 current study with a sensor grid that covers an area of approximately 500m by 500m with
 168 50m spacing between sensors, we set an upper limit of 5 times the spacing between sensors
 169 as the maximum cross-wind distance allowable between sources. If the sources are farther
 170 apart than this upper limit, they can be treated as individual single-source events in the
 171 present study. This reasoning also extends to sources that are extremely close to each other
 172 in the cross-wind direction, such that plumes overlap heavily to behave as a single source
 173 release. Therefore, a lower limit of one fifth of the spacing between sensors is used, below
 174 which we assume that plumes overlap and can be considered a single source release.

175 The additional parameters, d and φ , are used to calculate the location of the second
 176 source, (x_{s2}, y_{s2}) , relative to the reference source. Equations 13 and 14 show the conversion
 177 from polar to rectangular coordinates with respect to the location of the primary source. It
 178 is not necessary to specify a primary source prior to the sampling process, because a source
 179 location, (x_{s1}, y_{s1}) , is estimated from the MCMC sampling process, which will then serve as
 180 the reference source for other sources. Note that the other source locations are calculated
 181 using the estimated parameters d and φ . The polar configuration allows for additional
 182 sources to branch off of the primary source.

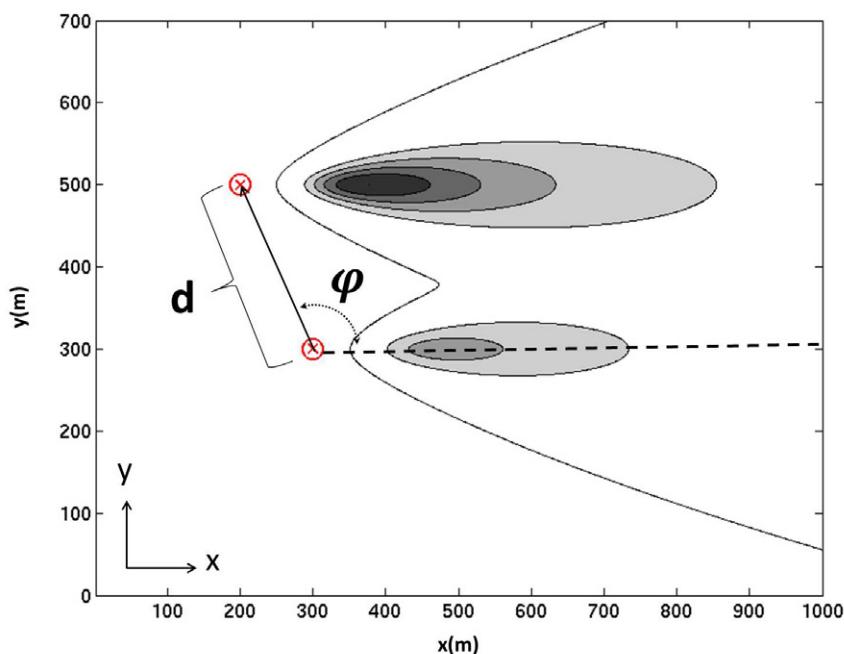


Figure 1. Sample dual source Gaussian plume colored by contaminant concentration at 2m above ground level. Source locations are shown as circles, d is the distance between sources, and φ is the angle between sources with respect to the positive x-axis.

$$x_{si} = x_{s1} + d_i \cos(\varphi_i) \quad (13)$$

$$y_{si} = y_{s1} + d_i \sin(\varphi_i) \quad (14)$$

183 where $i = 2, 3, \dots, N$ and N is the maximum number of possible sources.

184 4. Composite Ranking to Determine the Number of Sources

185 Concentration or dosage of contaminant measured at the sensors can be an outcome
 186 of releases from single or multiple sources. However, in the ER problem we do not know
 187 the number of sources involved in a dispersion event, even for a single source release. A
 188 concentration field resulting from a multiple source release can come close to matching a
 189 concentration field from a single source with a different emission rate and source location.

190 The Bayesian framework that we presented in the previous section does not provide any
 191 inference on the number of sources involved in a dispersion event. Therefore, we propose a
 192 composite ranking approach to estimate the number of sources involved in an event. The
 193 ranking system is independent of the Bayesian inference to locate the source and emission
 194 rate. We consider single, dual, and three-source releases, but the overall method is applicable
 195 to more than three sources. In our approach, we execute MERT for each release possibility
 196 independently. Once the runs are completed, we extract the most probable value for each of
 197 the model parameters from the corresponding posterior probability distributions. We then
 198 run the forward model using the most probable parameters to calculate the concentrations
 199 at each of the sensor locations. We designate these model concentrations as \hat{C} and compare
 200 them to the measured concentrations, C , for single, dual, and three-source assumptions
 201 separately using a ranking method.

202 In atmospheric dispersion applications, it is typical to use multiple performance metrics
 203 to effectively evaluate the predictive capability of a dispersion model. Researchers suggested
 204 a variety of metrics (Stohl et al., 1998; Pullen et al., 2005; Svensson, 1998; Chang et al., 2003;
 205 Hanna et al., 1993). We propose a composite ranking model that is inspired by the recent
 206 Environmental Protection Agency protocol to determine the best performing air quality
 207 model (EPA, 2012). The literature is mostly in agreement that error (scatter), bias, and
 208 correlation are important metrics in the evaluation process, all of which are included in some
 209 form in the global statistics portion of Mosca et al. (1998). Each of these metrics is weighted
 210 equally in our ranking model to decide whether a specific model achieves better results using
 211 a single or multiple source setting. We then identify the setting with the higher ranking as
 212 the release event containing the correct number of sources.

213 Our ranking model has three parts. The first component of the model's rank is the
 214 FAC2, which is a quantity measuring the fraction of predictions that fall within a factor
 215 of two of the corresponding observations (Chang et al., 2003), as shown in Equation 15 .
 216 This operation is performed to obtain a measure of error, or scatter, when comparing the
 217 observed and predicted values.

$$\text{FAC2} = \text{fraction of data for which } 0.5 \leq \frac{\hat{C}}{C} \leq 2.0, \quad (15)$$

218 where C is the observed concentration at the sensor and \hat{C} is the estimated concentration
 219 calculated by using the most probable parameters, obtained from posterior distributions, in
 220 the forward model.

221 The next performance metric used in the ranking model is the Fractional Bias (FB). The
 222 FB is used to indicate a bias towards underprediction or overprediction of concentration
 223 data by the model. It has been used as a validation parameter for other dispersion models
 224 and is a robust indicator of model performance (Stohl et al., 1998). The FB ranges from
 225 -2 (extreme underprediction) to +2 (extreme overprediction), and 0.0 is a perfect score for
 226 this component. As part of the United States Environmental Protection Agency's (EPA)
 227 performance evaluation protocol (EPA, 1992), the FB is defined as follows:

$$FB = 2 \left(\frac{\bar{C} - \bar{\hat{C}}}{\bar{C} + \bar{\hat{C}}} \right), \quad (16)$$

228 where \bar{C} is the average measured concentration across all sensors, and $\bar{\hat{C}}$ is the average of
 229 the predicted concentrations computed by the model at all sensor locations.

230 The final component to our ranking model is the Pearson's Correlation Coefficient (R),
 231 which contributes a measure of correlation to the ranking model. R ranges from -1.0 to +1.0
 232 with +1.0 corresponding to "perfect positive correlation" (EPA, 2012). An R value close to
 233 0.0 would indicate that the predicted data and the measured data are not related. R is
 234 defined as follows:

$$R = \frac{\sum_i (C_i - \bar{C}) \cdot (\hat{C}_i - \bar{\hat{C}})}{\left[\sqrt{\sum_i (C_i - \bar{C})^2} \right] \left[\sqrt{\sum_i (\hat{C}_i - \bar{\hat{C}})^2} \right]} \quad (17)$$

235 The three components described above are combined to form the following ranking model

$$RANK = FAC2 + \left(1 - \frac{|FB|}{2} \right) + R^2 \quad (18)$$

236 The ranking model contains a measure of error (scatter), bias, and correlation in a composite
 237 fashion. These metrics provide a concise and quantitative description of how well the model
 238 performs with a varying number of sources. The composite rank ranges from 0 to 3, with
 239 3 corresponding to a perfect score. The higher the *RANK*, the better the model did at
 240 matching the concentration predictions with sensor observations. We use the highest ranking
 241 model to make a decision on the correct number of sources involved in the dispersion event.

242 5. Results

243 In 2007, the Defense Threat Reduction Agency (DTRA) proceeded to address some of
 244 the unmet requirements in the current Joint Effects Model (JEM), which is to be used as the
 245 standard hazard prediction model at the Department of Defense (Storwold Jr., 2007). One
 246 of these requirements was to evaluate source term estimation models used to detect chemical
 247 and biological (CB) activity and estimate the characteristics of the source(s) in question. A
 248 large data set, FFT-07, was created for the evaluation and improvement of STE algorithms.
 249 The FFT-07 database provides detailed meteorological information and trace gas concentra-
 250 tion measurements for short range (500m) dispersion experiments. These experiments were
 251 performed with single and multiple sources for continuous and puff (instantaneous) releases.

252 5.1. Evaluation with FFT-07 Trials

253 We use data from Trials 7, 27, 28, and 40 of FFT-07. In trials 27 and 40, there are two
 254 sources with different tracer emission rates. Trial 7 is a single source trial that we include

255 in our study to demonstrate that the ranking model will identify the correct number of
256 source terms, even in a single source case. Trial 28 is a three source case. The true source
257 locations and emission rates are known from the field data and used to assess the accuracy
258 of the reconstructed model parameters. In working with the FFT-07 concentration data, we
259 ignored sensor data that reports an error message for more than 50% of the sampling time.

260 In FFT-07, a grid of 100 digital photoionization detectors (digiPID) were spaced evenly
261 on a square grid at 50m apart and 2m above the ground. A tracer of propylene gas was
262 released from multiple locations at approximately 2m above ground and at constant flow
263 rates for approximately 15 minutes per trial. We time-averaged the concentration data from
264 sensors for the continuous release trials, which are the focus of the present study.

265 FFT-07 Trial 40 had very few poor readings (sensors reporting an error more than 50% of
266 the time). This abundance of reliable sensor data and fairly uniform wind conditions resulted
267 in reconstructions of the source locations that are approximately 8 and 6 meters from the
268 true source locations, as seen in Figure 2. For this case, 48 of the 100 sensors are used in
269 the estimation. Note that we include all positive reading sensors. Figure 3 shows the tight
270 posterior distributions for the two source locations in which the true values fall within, or
271 very close to, the 50% contour line. This inner contour line encompasses 50% of the posterior
272 samples and the outer contour line includes 90% of the posterior samples. The range of each
273 cell is normalized in both the horizontal and vertical direction with the limits corresponding
274 to the minimum and maximum values for each parameter in the posterior samples. The
275 normalization enables us to assess accuracy in percentage form in a global fashion over the
276 parameter space. The plots along the diagonal show the marginal distributions of each
277 parameter. Trial 40 is a good example of successful reconstruction from reliable sensor data.

278 Figure 4 shows a comparison of results from FFT Trial 40, where the left image uses a
279 single source setting, the middle uses a dual source setting, and the third image uses a three
280 source setting. The predicted values for the dual source setting (middle) match more closely
281 to the data measured by the sensors. A perfect match would lie directly on the solid diagonal
282 line running through the origin. This view of the data allows us to see the difference between
283 an estimate with a single, dual, an three source setting. It also shows the points which fall
284 within a factor of two of the observed values (FAC2) as well as the over or underestimation
285 (Bias). From this figure, we can visually deduce that the dual source setting is most likely
286 the correct answer, but we need a quantitative measure. Therefore, we proposed a composite
287 ranking model as described in Section 4.

288 The more reliable the sensor data, the more accurate the reconstruction will be. However,
289 operational data may be less reliable than desired. Hence we use Trial 27 from the FFT-07
290 data set, which has much less reliable data than the Trial 40, to test how less reliable or
291 sparse data affects the reconstruction.

292 Figure 5 shows the layout of the 57 sensors used in Trial 27, as well as the true and
293 estimated source locations. We observe that the most probable source locations are approx-
294 imately 15 and 25 meters from the true source locations. The true source locations are
295 illustrated with squares and the source location estimates with \times 's. Ideally, the estimates
296 would fall directly on the true locations (e.g. \times 's on top of squares). The distances may not

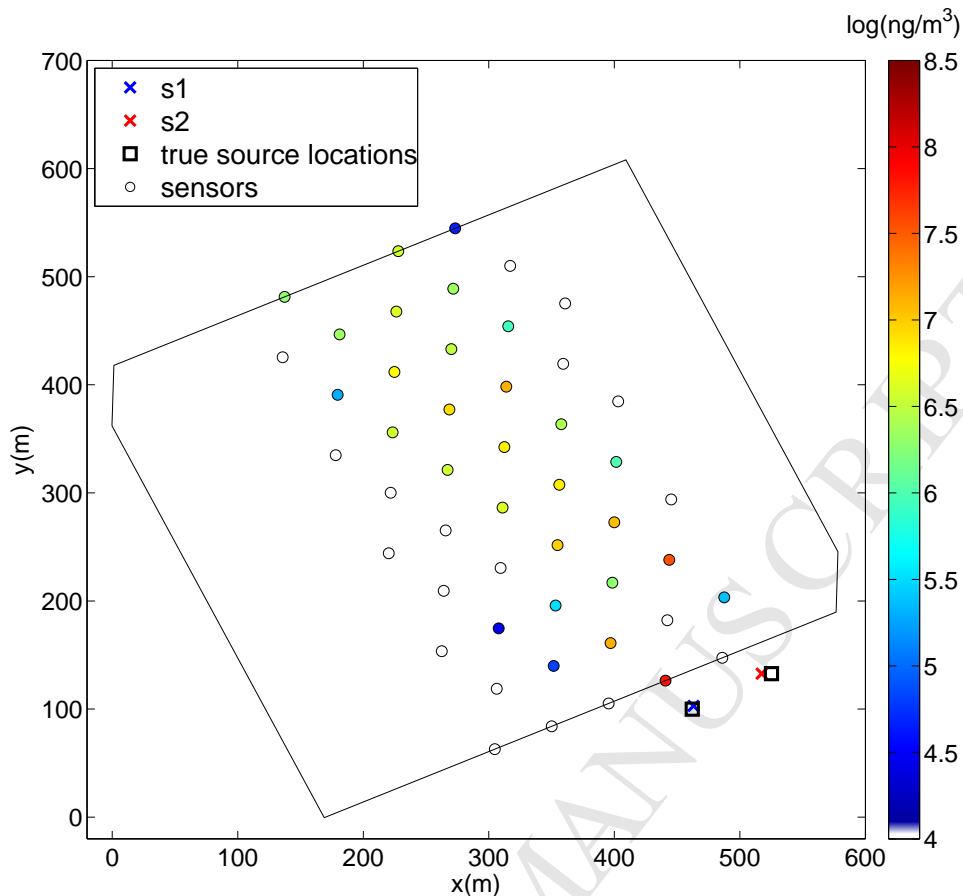


Figure 2. FFT-07 Trial 40 source location estimates (s1 and s2) with approximate errors of 8m and 6m. Sensors reporting nominally zero concentration are colored white. Large rotated box is the FFT-07 sensor network boundary.

297 be ideal (and not as small as Trial 40), but can still be very useful from an operational point
 298 of view since they would at least put any rapid response personnel in close proximity to the
 299 true locations.

300 FFT-07 Trial 28 is a three-source release event and a similar layout plot can be seen in
 301 Fig. 6. In this figure we can see that estimated source locations for sources 1 and 3 are fairly
 302 close to the true values, but the estimated source location for source 2 is approximately 48m
 303 from the true source location. We do note, however, the estimated sources are in a somewhat
 304 linear arrangement, as are the true source locations, and they are of approximately correct
 305 spacing with respect to one another.

306 5.2. Composite Ranking Model Results

307 Thus far, we have presented reconstruction of source locations and emission rates for dual
 308 and three-source releases. We have not made an attempt to estimate the number of sources
 309 involved in a dispersion event. The composite ranking model that we proposed in Section 4

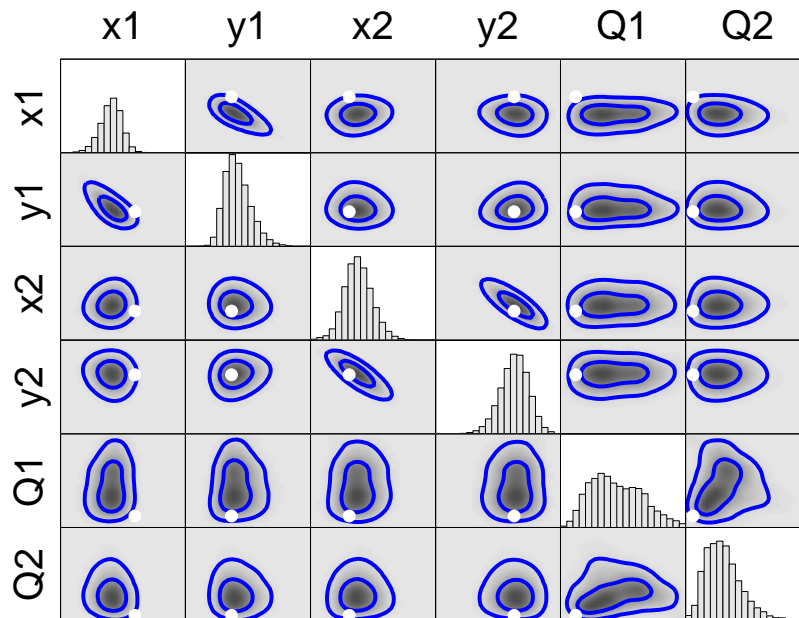


Figure 3. FFT-07 Trial 40 bivariate posterior distributions for location and emission strength. The range of each cell is normalized with respect to the minimum and maximum values for each parameter and distances can be viewed as percent error. The plot is colored by probability density and the darkest regions are the most probable. The outer contour encompasses 90% of the posterior samples and the inner contour includes 50%. White markers represent true values.

310 enables us to estimate the number of sources. We calculate *RANK* using Equation 18. The
 311 components that make up the *RANK* are: *FAC2*, *FB*, and *R*.

312 Figure 7 shows the composite ranking for all cases in this study, and is colored by con-
 313 tribution from each component in the rank. A rank of 3.0 corresponds to a perfect score.
 314 For all the cases tested, the model with the correct number of sources ranked higher. For
 315 instance, Trial 7 is a single source release, and our ranking model gives the highest score
 316 to the single source assumption correctly. In all the other cases the correct source-number
 317 assumption received the highest score, as expected.

318 6. Conclusions

319 We have extended a Bayesian inference method to reconstruct single-source contaminant
 320 release event, SERT, to reconstruct near-ground-level multiple-source release events, MERT.
 321 We proposed a composite ranking system to identify the number of sources involved in an
 322 event. The ranking formula is independent of the Bayesian method and can potentially be
 323 adopted in other event reconstruction methods.

324 We have applied the combined approach to releases from up to three sources, but the
 325 method can be extended to more than three sources. In the Bayesian framework we used a
 326 data-driven Gaussian plume model where turbulent diffusion parameters are inferred given
 327 the concentration data. The practice significantly improves the performance of the standard

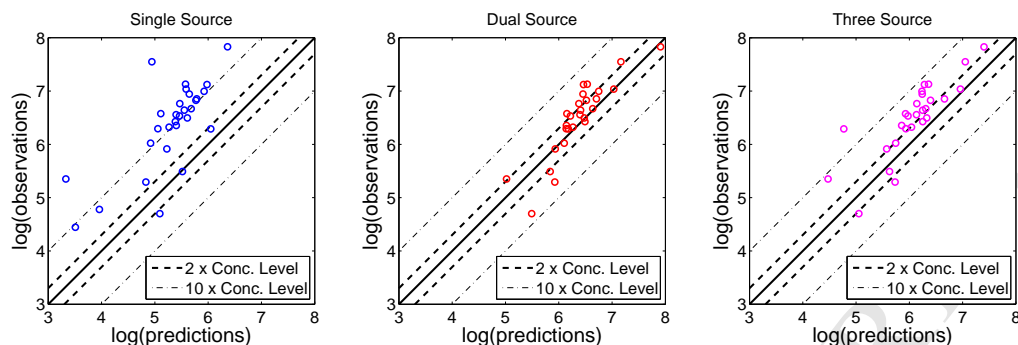


Figure 4. Observed sensor concentrations for FFT-07 Trial 40 vs. computed sensor concentrations using the most probable model parameters.

328 Gaussian plume model. However, for complicated dispersion events, sophisticated dispersion
 329 models should be preferred as the forward model.

330 Acknowledgments

331 This work is supported by a grant from the U.S. National Science Foundation (Award
 332 #1043107). Authors would like to thank the anonymous reviewer for his contribution to the
 333 final form of the composite ranking formula.

334 References

- 335 Akcelik, V., Biros, G., Draganescu, A., Hill, J., Ghattas, O., Waanders, B., 2005. Dynamic data-driven inver-
 336 sion for terascale simulations: Real-time identification of airborne contaminants, in: SC '05 Proceedings
 337 of the 2005 ACM/IEEE conference on Supercomputing.
- 338 Allen, C.T., Young, G.S., Haupt, S.E., 2007. Improving pollutant source characterization by better estimating
 339 wind direction with a genetic algorithm. *Atmospheric Environment* 41, 2283–2289.
- 340 Annunzio, A., Young, G., Haupt, S., 2012a. A multi-entity field approximation to determine the source
 341 location of multiple atmospheric contaminant releases. *Atmospheric Environment* 62, 593–604.
- 342 Annunzio, A., Young, G., Haupt, S., 2012b. Utilizing state estimation to determine the source location for
 343 a contaminant. *Atmospheric Environment* 46, 580–589.
- 344 Chang, J., Franzese, P., Chayantrakom, K., Hanna, S., 2003. Evaluations of CALPUFF, HPAC, and VL-
 345 STRACK with two mesoscale field datasets. *Journal of Applied Meteorology* 42, 453–466.
- 346 Chow, F., Kosovic, B., Chan, S., 2008. Source inversion for contaminant plume dispersion in urban environ-
 347 ments using building-resolving simulations. *Journal of Applied Meteorology and Climatology* 47.
- 348 Congdon, P., 2010. *Applied Bayesian Hierarchical Methods*. Chapman and Hall/CRC.
- 349 EPA, 1992. Protocol for Determining the Best Performing Model. Technical Report EPA-454/R-92-025.
 350 United States Environmental Protection Agency.

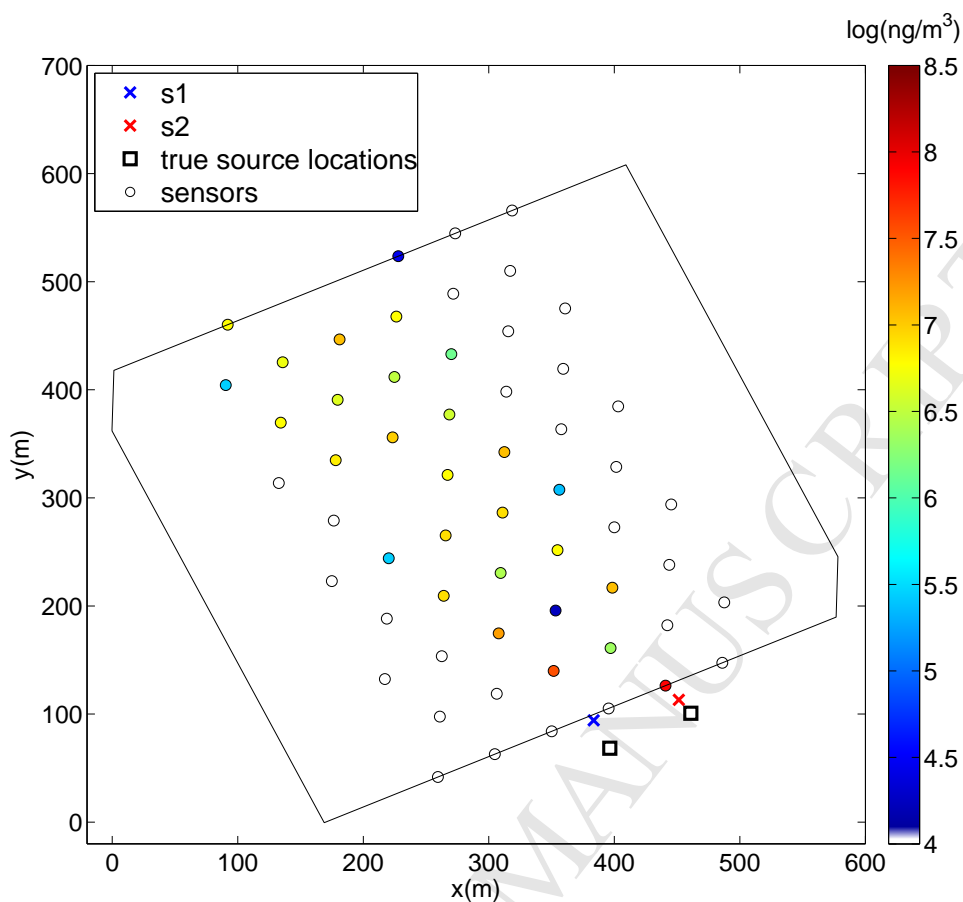


Figure 5. FFT-07 Trial 27 source location estimates (s1 and s2) with approximate errors of 15m and 25m. Sensors reporting nominally zero concentration are colored white. Large rotated box is the FFT-07 sensor network boundary.

- 351 EPA, 2012. Documentation of the Evaluation of CALPUFF and Other Long Range Transport Models
 352 Using Tracer Field Experiment Data. Technical Report EPA-454/R-12-003. United States Environmental
 353 Protection Agency.
- 354 Hanna, S., Briggs, G., Hosker Jr., R., 1982. Handbook on Atmospheric Diffusion. U.S. Department of
 355 Energy: Office of Energy Research. doe/tic-11223 edition.
- 356 Hanna, S., Chang, J., Strimaitis, D., 1993. Hazardous gas model evaluation with field observations. *Atmo-*
 357 *spheric Environment* 27A, 2265–2285.
- 358 Henze, D., Seinfeld, J., Shindell, D., 2009. Inverse modeling and mapping US air quality influences of
 359 inorganic $PM_{2.5}$ precursor emissions using the adjoint of GEOS-Chem. *Atmospheric Chemistry and*
 360 *Physics* 9, 5877–5903.
- 361 Johannesson, G., Hanley, B., Nitao, J., 2004. Dynamic Bayesian Models via Monte Carlo - An Introduction
 362 with Examples. Technical Report UCRL-TR-207173. Lawrence Livermore National Laboratory.
- 363 Keats, A., Yee, E., Lien, F., 2007. Bayesian inference for source determination with applications to a complex
 364 urban environment. *Atmospheric Environment* 41, 465–479.
- 365 Metropolis, N., Rosenbluth, A., Rosenbluth, M., Teller, E., 1953. Equations of state calculations by fast

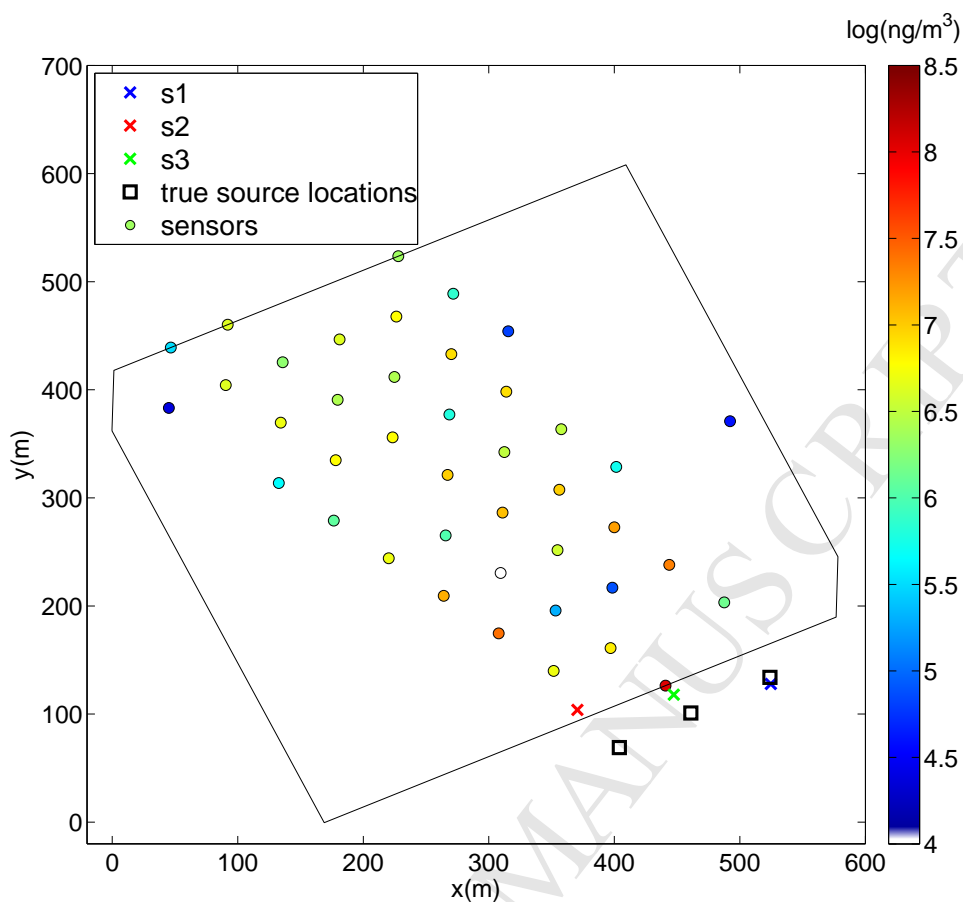


Figure 6. FFT-07 Trial 28 source location estimates (s1, s2, and s3) with approximate errors of 7.5m, 21.7m, and 48.3m, respectively. Sensors reporting nominally zero concentration are colored white. Large rotated box is the FFT-07 sensor network boundary.

- 366 computing machines. *Journal of Chemical Physics* 224, 560–586.
- 367 Monache, L.D., Lundquist, J., Kosovic, B., Johannesson, G., Dyer, K., Aines, R., Chow, F., Belles, R.,
 368 Hanley, W., Larsen, S., Loosmore, G., Nitao, J., Sugiyama, G., Vogt, P., 2008. Bayesian inference and
 369 markov chain monte carlo sampling to reconstruct a contaminant source on a continental scale. *Journal*
 370 *of Applied Meteorology and Climatology* 47, 2600–2613.
- 371 Mosca, S., Graziani, G., Klug, W., Bellasio, R., Bianconi, R., 1998. A statistical methodology for the evalu-
 372 ation of long-range dispersion models: An application to the ETEX exercise. *Atmospheric Environment*
 373 32, 4307–4324.
- 374 Platt, N., DeRiggi, D., 2010. Comparative investigation of source term estimation algorithms using FUSION
 375 field trial 2007 data. *AMS 16th Conference on Air Pollution Meteorology* .
- 376 Platt, N., DeRiggi, D., 2012. Comparative investigation of source term estimation algorithms using FUSION
 377 field trial 2007 data: linear regression analysis. *International Journal of Environment and Pollution* .
- 378 Pullen, J., Boris, J., Young, T., Patnaik, G., Iselin, J., 2005. A comparison of contaminant plume statistics
 379 from a gaussian puff and urban CFD model for two large cities. *Atmospheric Environment* 39, 1049–1068.
- 380 Senocak, I., 2010. Application of a bayesian inference method to reconstruct short-range atmospheric disper-

- 381 sion events, in: Bayesian Inference and Maximum Entropy Methods in Science and Engineering, American
382 Institute of Physics, Chamonix, France.
- 383 Senocak, I., Hengartner, N., Short, M., Daniel, W., 2008. Stochastic event reconstruction of atmospheric
384 contaminant dispersion using bayesian inference. *Atmospheric Environment* 42, 7718–7727.
- 385 Stockie, J., 2011. The mathematics of atmospheric dispersion modeling. *SIAM Review* .
- 386 Stohl, A., Hittenberger, M., Wotawa, G., 1998. Validation of the lagrangian particle dispersion model flexpart
387 against large-scale tracer experiment data. *Atmospheric Environment* 32, 4245–4264.
- 388 Storwold Jr., D., 2007. Detailed Test Plan for the FUsing Sensor Information from Observing Networks
389 (FUSION) Field Trial 2007 (FFT-07). Technical Report WDTC-TP-07-078. United States Army.
- 390 Svensson, G., 1998. Model simulations of the air quality in athens, greece, during the MEDCAPHOT-TRACE
391 campaign. *Atmospheric Environment* 32, 2239–2268.
- 392 Watson, J., Chow, J., 2004. Receptor models for air quality managment. *Environmental Management* ,
393 27–36.
- 394 Yee, E., 2008. Theory for reconstruction of an unknown number of contaminant sources using probabilistic
395 inference. *Boundary-Layer Meteorology* 127, 359–394.
- 396 Yee, E., 2012a. Inverse dispersion for an unknown number of sources: Model selection and uncertainty
397 analysis. *ISRN Applied Mathematics* .
- 398 Yee, E., 2012b. Probability theory as logic: Data assimilation for multiple source reconstruction. *Pure and*
399 *Applied Geophysics* 169, 499–517.

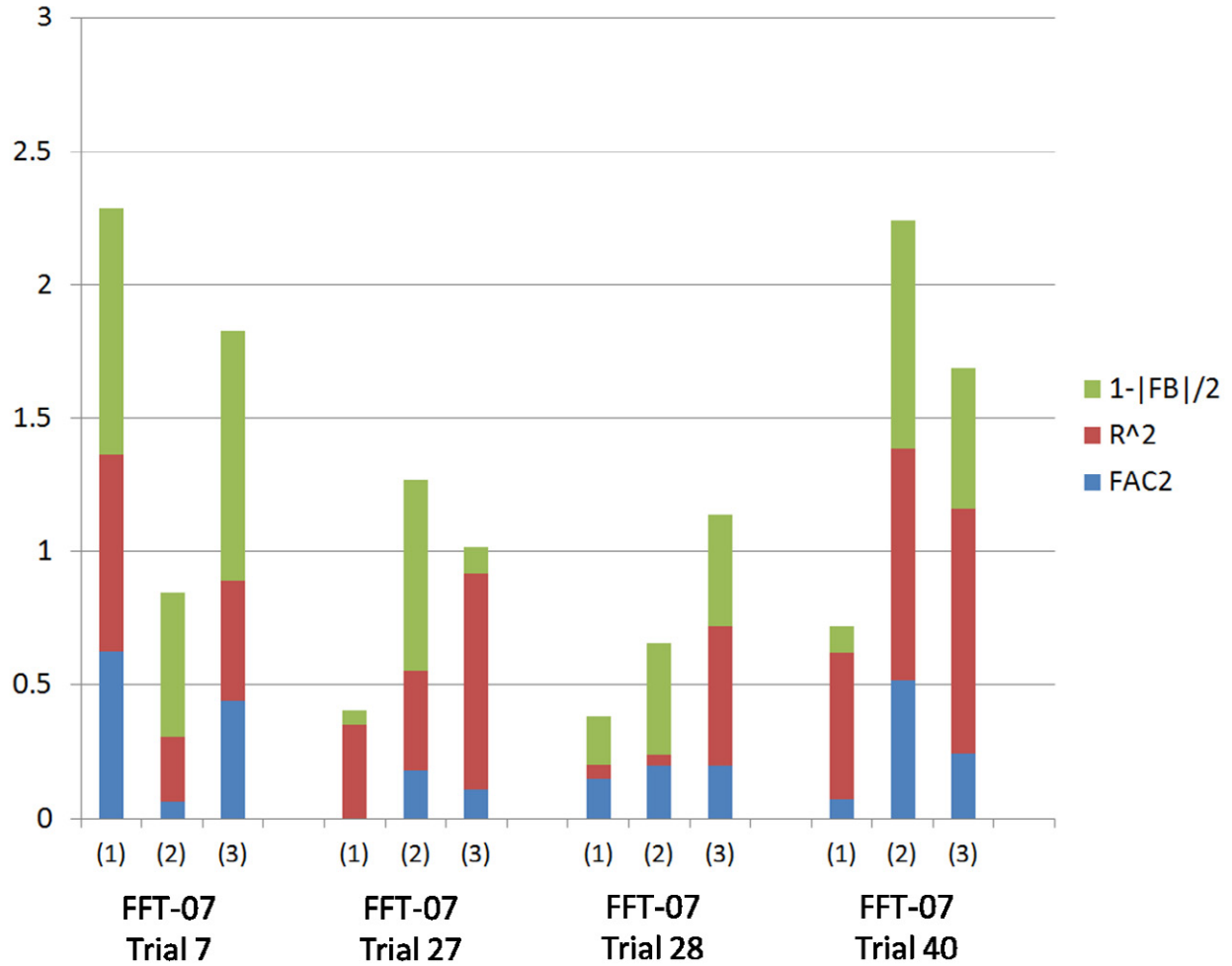


Figure 7. Ranking for each case tested. Colors correspond to individual rank components (e.g. R^2 , FAC2, $1 - |FB|/2$) as shown in legend. (1),(2),(3) refer to single, dual, and three source settings, respectively. FFT-07 Trials 27 and 40 are truly dual source releases. Trial 7 is a single source release and Trial 28 is a three source release.